EUROPEAN JOURNAL OF CANCER 48 (2012) 129–137

available at www.sciencedirect.com

ScienceDirect

journal homepage: www.ejconline.com

Human adipose tissue-derived mesenchymal stem cells: Characteristics and therapeutic potential as cellular vehicles for prodrug gene therapy against brainstem gliomas

Seung Ah Choi [a], *Ji Yeoun Lee* [a], *Kyu-Chang Wang* [a], *Ji Hoon Phi* [a], *Sang Hoon Song* [b], *Junghan Song* [b], *Seung-Ki Kim* [a,*]

[a] *Division of Pediatric Neurosurgery, Seoul National University Children's Hospital, Seoul National University College of Medicine, Seoul, Republic of Korea*

[b] *Department of Laboratory Medicine, Seoul National University Bundang Hospital, Gyeong gi-do, Republic of Korea*

ARTICLE INFO

Article history:
Available online 12 June 2011

Keywords:
Adipose tissue-derived mesenchymal stem cells
Brainstem glioma
Prodrug gene therapy
Carboxylesterase

ABSTRACT

Human mesenchymal stem cells (hMSCs) have emerged as attractive cellular vehicles for gene therapy against brain malignancy because of their targeted tropism for cancer and the intrinsic attribute of autologous transplantation. We evaluated the characteristics and therapeutic potential of human adipose tissue-derived MSCs (hAT-MSCs) and prodrug gene therapy against diffuse pontine gliomas.

The hAT-MSCs were isolated from human adipose tissue and characterised for morphology, surface markers and potential to differentiate into mesenchymal and neuronal lineages. We genetically modified hAT-MSCs to express rabbit carboxylesterase (rCE) enzyme, which can efficiently convert the prodrug CPT-11 (irinotecan-7-ethyl-10-[4-(1-piperidino)-1-piperidino]carbonyloxycamptothecin), into the active drug SN-38 (7-ethyl-10-hydroxycamptothecin). The migratory capacity of hAT-MSCs expressing rCE (hAT-MSC.rCE), their ability to convert CPT-11 to SN-38 and cytotoxic effect on F98 cells were evaluated *in vitro*. The therapeutic potential of hAT-MSC.rCE was confirmed using a rat brainstem glioma model.

The hAT-MSCs showed fibroblast-like morphology and expressed hMSC-specific markers including CD73, CD90 and CD105. The hAT-MSCs could differentiate into a mesenchymal lineage and transdifferentiate into a neuronal lineage under optimum culture conditions. The hAT-MSC.rCE converted CPT-11 to SN-38 and preserved the tumour tropism of hAT-MSCs. Brainstem glioma-bearing rats treated with hAT-MSC.rCE and CPT-11 survived 5 d more than rats treated with CPT-11 only ($p = 0.0018$).

Our study demonstrates that hAT-MSCs can be easily prepared and genetically modified as cellular vehicles for prodrug gene therapy and that they have therapeutic potential against brainstem gliomas.

1. Introduction

Brainstem gliomas are one of the most malignant and dismal cancers in children. These tumours are primarily treated with radiation therapy. However, 1- and 5-year progression-free survival rates are less than 25% and 10%, respectively.[1,2] Therefore, there is substantial need for the development of novel strategies for children with brainstem gliomas.

* *Corresponding author:* Address: Division of Pediatric Neurosurgery, Seoul National University Children's Hospital, 101 Daehak-ro, Jongno-gu, Seoul 110-744, Republic of Korea. Tel.: +82 2 2072 3084; fax: +82 2 744 8459.
E-mail address: nsthomas@snu.ac.kr (S.-K. Kim).

0959-8049/$ - see front matter © 2011 Elsevier Ltd. All rights reserved.
doi:10.1016/j.ejca.2011.04.033

Stem cells have been suggested as vehicles for brain tumour therapy.[3,4] Neural stem cells (NSCs) are prototypes of stem cell based gene therapy.[3,5,6] Recently The US Food and Drug Administration has approved City of Hope researchers (Dr. Aboody/Dr. Portnow), to conduct the first-in-human study of a neural stem cell-based therapy targeting recurrent high-grade glioma (http://www.clinicaltrials.gov/ct2/show/NCT01172964?term=Neural+stem+cells+%26+glioma&rank= 1). However, the clinical application of NSCs is not always feasible because of ethical and logistic problems related to their isolation. In this context, mesenchymal stem cells (MSCs) have been considered as alternative cellular vehicles.[7,8] In addition to the capacity to migrate to brain tumours,[9] compared to that of NSCs, MSCs are easily attainable in large quantities from diverse sources without any ethical conflicts or immunological considerations.[10] Furthermore, hMSCs possess an extensive proliferative potential and the capacity to differentiate into various cell types.[7,8,10,11]

Recently MSCs from human adipose tissues has emerged as an attractive source for autologous MSC therapy because of the easy and repeatable access to subcutaneous adipose tissue, simple isolation procedure and high yield of MSCs.[12,13] Our previous works confirmed an extensive migratory capacity and therapeutic potential of genetically modified human adipose tissue-derived MSCs (hAT-MSCs) for experimental brain tumours.[9,14] In MSC-based gene therapy, the gene-directed enzyme prodrug strategy is ideal because the MSCs can provide agents that kill tumour cells as well as themselves if the MSCs proliferate *in vivo*.[13,15] We adopted MSCs producing rabbit carboxylesterase (rCE) and systemic administration of CPT-11 (irinotecan-7-ethyl-10-[4-(1-piperidino)-1-piperidino]carbonyloxycamptothecin) as the therapeutic proof-of-concept. Activation of CPT-11 by human esterase is poor, whereas the rCE converts the prodrug CPT-11 more efficiently into the cytotoxic drug SN-38 (7-ethyl-10-hydroxycamptothecin), a potent topoisomerase I inhibitor.[16,17]

In the present study, we isolated and characterised MSCs from the human adipose tissues. We also evaluated the therapeutic potential of hAT-MSCs for prodrug gene therapy against diffuse pontine gliomas.

2. Materials and methods

2.1. Cell culture

The hAT-MSCs were isolated from the abdominal fat prepared for sellar floor reconstruction in patients who underwent transsphenoidal surgery. Preparation of MSCs from fat tissues was approved by the institutional review board of the Seoul National University Hospital. All eligible patients or their parents provided written informed consent, and all samples were processed within 4 h. The adipose tissues were chopped and then treated with 0.075% collagenase (Sigma–Aldrich, St. Louis, MO) in phosphate buffered saline (PBS) at 37 °C for 1 h. The mononuclear cells were plated and cultured in MSC expansion medium (Chemicon, Temecula, CA) supplemented with 10% foetal bovine serum and 1% antibiotic–antimycotic solution (Invitrogen, Grand Island, NY). The hAT-MSCs were used for further experiments before passage 5. The rat glioma cell line F98 cells (American Type Culture Collection, Manassas, VA) were cultured in Dulbecco's modified Eagle's medium (DMEM; WelGene Biopharmaceuticals, Daegu, Korea) supplemented with 10% foetal bovine serum and 1% antibiotic–antimycotic solution. Cells were maintained at 37 °C in an incubator in a 5% CO_2/95% air atmosphere.

2.2. Fluorescence-activated cell sorting (FACS) analysis

The hAT-MSCs were characterised using cell surface markers by fluorescence-activated cell sorting (FACS) analyses. Cultured cells were detached in TryPLE express (Invitrogen) and washed in flow cytometry buffer (FCB; 2% FBS, 0.2% Tween-20 in PBS). The hAT-MSCs were labelled with fluorescein-isothiocyanate (FITC)-conjugated monoclonal antibodies directed against cluster of differentiation (CD) markers, including CD14 (BD Biosciences Pharmingen, San Diego, CA), CD90 (BD Biosciences Pharmingen) and CD105 (Chemicon), or they were labelled with phycoerythrin (PE)-conjugated monoclonal antibodies directed against CD34 (BD Biosciences Pharmingen), CD45 (Chemicon), and CD73 (BD Biosciences Pharmingen). Analysis was performed using a FACscan argon laser cytometer (Becton Dickinson, San Jose, CA).

2.3. In vitro mesenchymal differentiation of hAT-MSCs

To confirm the multipotency of hAT-MSCs, differentiation assays were performed. hAT-MSCs were stimulated in three different appropriate induction media using the mesenchymal differentiation kit (Invitrogen).[14] For adipogenic, chondrogenic and osteogenic differentiation, cells were treated in induction medium for 2 or 3 weeks with medium changes 3 times per week. Then, the cells were stained with oil red O for adipogenic differentiation (Sigma–Aldrich), alcian blue for chondrogenic differentiation (Sigma–Aldrich) or alizarin red S for osteogenic differentiation (Sigma–Aldrich), respectively. Unstimulated cells and cells treated with identical amounts of diluents were used as controls. After being washed, cells were visualised by light microscopy.

2.4. In vitro neuronal differentiation of hAT-MSCs

hAT-MSCs were induced into neuronal differentiation by serum-free neurobasal media with 20 ng/mL basic fibroblast growth factor (bFGF; Millipore, Billerica, MA) and 20 ng/mL human epithelial growth factor (hEGF; Millipore) for 72 h. The formation of floating bodies was observed within 7 d. For neuronal induction, spheres were dissociated and seeded onto Lab-Tek chamber slides (Nunc International, Rochester, NY) in DMEM/2% FBS, 100 ng/mL bFGF for 14 d. The immunophenotype of hAT-MSCs was evaluated using primary antibodies directed against neuronal class III β-tubulin (Tuj1, used as a neuronal marker, 1:500; Covance, Berkeley, CA), glial fibrillary acidic protein (GFAP, used as an astrocyte marker, 1:500; Covance), and O4 (used as an oligodendrocyte marker, 1:100; Chemicon). The secondary antibody Alexa Fluor 488-conjugated goat anti-mouse IgG (1:200; Invitrogen) was used after washing. Cells were mounted with antifading solution containing 4-6-diamidino-2-phenylindole (DAPI; Vector Laboratories, Burlingame, CA). The cells were observed using a confocal microscope (Zeiss, Oberkochen, Germany).

2.5. Engineering of hAT-MSC.rCE

To construct the hAT-MSCs expressing rCE (hAT-MSC.rCE), the pIRES2.GFP (5.3 kb) vector containing Kan/Neo resistance gene was purchased from BD Biosciences Clontech (San Jose, CA), and the *rCE* cDNA was obtained courtesy of M.K. Danks (St. Jude Children's Research Hospital, Memphis, TN). *rCE* (1751 bp) was inserted into the EcoRI/SalI (Invitrogen) cloning site of pIRES2.GFP. Nucleofection was performed using the Nucleofector II device (Amaxa Biosystem, Lonza, Cologne, Germany) according to the manufacturer's instructions with some modifications. Cells (5×10^5) were resuspended in 100 μL of Nucleofector buffer (Amaxa Biosystems) with 3 μg of plasmid DNA. For high efficiency, program U-23 was used. Nucleofected cells were immediately plated onto six-well plates. To remove dead cells, the medium was changed 5 h after nucleofection. After transfection of hAT-MSCs with the rCE (or vector alone as a control), transfectants were selected with G418. Expression of green fluorescent protein (GFP) was observed by fluorescence microscopy 72 h after nucleofection. Transfection efficiency was analysed by the expression of GFP using FACS analysis 7 d after nucleofection and immediately before *in vivo* injection. Cells were dissociated with TryPLE (Invitrogen) and washed. Then, cells were resuspended in flow cytometry buffer containing 1% FBS and sorted using a FACSAria Flow cytometer (BD Biosciences). Non-specific fluorescence was eliminated by selecting hAT-MSCs that were not transfected with GFP.

2.6. Reverse transcription polymerase chain reaction (RT-PCR)

Total RNA from hAT-MSCs and hAT-MSC.rCE was extracted with the TRIzol reagent (Invitrogen) and cDNA was synthesised using primescript™ RT-PCR kit (Takara, Shiga, Japan) according to the manufacturer's instructions. PCR was conducted with Accupower PCR Premix (Bioneer, Daejeon, Korea), followed by 30 PCR amplification cycles (94 °C for 30 s, annealing at 55 °C for 60 s, and extension at 72 °C for 90 s). The sense and antisense primers of the RT-PCR reaction were as follows: *rCE*, sense: 5-GCGAATTCATGTGGCTCTGTGCATTGGCC-3, antisense: 5-GCCGTCGACTCACAGCTCAATGTGCTCTG-3 (1751 bp amplicon) and *GAPDH*, sense: 5-CGTGGAAGGA CTCATGAC-3, antisense: 5-CAATTCGTTGTCATACCAG-3 (513 bp amplicon). The PCR products were analysed by electrophoresis on 1% agarose gels, stained with ethidium bromide and visualised using a UV transilluminator.

2.7. CPT-11 conversion assay

Conversion of CPT-11 to SN-38 was monitored in the conditioned media of hAT-MSCs and hAT-MSC.rCE. The conditioned medium was harvested after incubation of 2×10^5 cells with 5 μM of CPT-11 (CJ Cheiljedang Corp, Seoul, Korea) for 72 h in 50 mM HEPES (pH 7.4, Invitrogen) at 37 °C in 5% CO_2. The concentration of SN-38 was measured by high performance liquid chromatography-tandem mass spectrometry (HPLC-MS/MS). Briefly, mixed solutions of CPT-11 and SN-38 of 0–300 ng/ml in acetonitrile with 20 mM ammonium acetate were used as standards. For the internal standard, 500 ng/ml of SN-38 (Sigma–Aldrich, St. Louis, MO) in DMSO–methanol (50:50, v/v) was used. The internal standard (0.1 ml) and the sample were mixed and centrifuged for 3 min. The supernatant (0.1 ml) was mixed with 0.1 ml of acetonitrile with 20 mM ammonium acetate. The mixture was centrifuged for 3 min, and the resulting supernatant was transferred to the autosampler of the liquid chromatography apparatus. The concentrations of CPT-11 and SN-38 were measured with the multiple reaction monitoring (MRM) function of the mass spectrometer.

2.8. In vitro bioactivity of CPT-11

The hAT-MSCs and hAT-MSC.rCE (4×10^3/ per well each) were seeded in 96-well plates and treated with various concentrations of CPT-11 (0, 1, 3, 5, 7, 10, 20, or 50 μM), which was converted to SN-38 by rCE. Cells were incubated for 3 d, and cell viability was measured using a colorimetric assay (Cell Counting Kit-8 (CCK); Dojindo Molecular Technologies, Kumamoto, Japan). All experiments were conducted in triplicate. Experimental values were expressed as the mean percentage of control viability ± standard error of the mean (SEM).

2.9. In vitro mixed co-culture

The therapeutic efficacy of hAT-MSC.rCE after CPT-11 treatment was analysed by coculture experiments. F98 cells (4×10^3 per well) were seeded in 96-well plates and the experiments were done as follows: on day 1, hAT-MSCs or hAT-MSC.CE cells (8 10^3 per well) were added to the tumour cell cultures; on day 2, CPT-11 (0, 3, 5, 7 or 10 μM) was added to the mixed cell cultures; on day 5, cell viability was quantified with colorimetric assays using the Cell Counting Kit-8. All experiments were done in triplicate. Experimental values were expressed as the mean percentage of control viability ± SEM.

2.10. In vitro migration assay

The migratory ability of hAT-MSCs and hAT-MSC.rCE towards F98 cells was determined using Transwell plates (Corning Costar, NY, USA) that were 6.5 mm in diameter with 8 μm pore filters. F98 cells (5×10^4/0.5 ml) were incubated in serum-free medium for 24 h and placed in the lower well. Serum-free medium served as the negative control for trigger factors. The hAT-MSCs or hAT-MSC.rCE (5×10^4/0.5 ml) were suspended in serum-free medium and seeded into the upper well. HFF-1 cells (a human fibroblast cell line from ATCC) were used as the negative control for migrating cells. After incubation for 6 h at 37 °C, the non-migratory cells were removed from the upper side of the filter and scraped off with a cotton swab. The filters were then stained with the Three-Step Stain Set (Diff-Quik; Sysmex) to confirm the migratory cells. The migration to the lower side of the filter was observed with a light microscope. Five high-power fields (×40) were scored. Stained cells were soaked in ice-cold acetic acid, oscillated for 10 min and then assessed by absorbance at 570 nm wavelength using a microplate reader. Experiments were performed in triplicate, and the values were expressed as means ± SEM.

2.11. *In vivo survival study*

All animal studies were carried out at the animal facility of the Seoul National University Hospital in accordance with national and institutional guidelines. Female Fischer 344 rats (150–200 g, Central Lab Animal, Seoul, Korea) were used and anesthetised with an intramuscular injection of a solution of 20 mg/kg Zoletil (Virbac, Carros, France) and 10 mg/kg xylazine (Bayer Korea, Seoul, Korea). The rat brainstem glioma model was followed as described previously.[9,18] F98 tumour cells (50,000 cells in 3 μl; $n = 32$) were implanted with a needle at an injection rate of 1 μl/min. Two days after the implantation of the tumour cells, the animals were randomised into four groups ($n = 8$ in each group): Group 1 and 2 were treated with an intratumoural injection of PBS (3 μl); Groups 3 and 4 were treated with an intratumoural injection of 200,000 hAT-MSC.rCE in 3 μl of PBS. In this study, hAT-MSC.rCE were labelled with the CM-DiI cell tracker prior to injection and injected twice. Two days after hAT-MSC.rCE injection, Groups 2 and 4 received intravenous injections of CPT-11 (7.5 mg/kg) for 12 d (5 d followed by a rest of 1 d). Discomfort or distress was assessed by animal care personnel with no knowledge of the protocol design. All euthanised rats were verified as tumour-bearing by necropsy. The end-point for the therapeutic study was long-term survival.

2.12. *In vivo histological analysis*

Whole brains of dead rats were harvested and fixed with 4% paraformaldehyde. The brains were dehydrated using elevated concentrations of sucrose and embedded in optimum cutting temperature compound (Tissue-Tek, Torrance, CA). The brains were stored at –80 °C, then sectioned using cryostat into 10 μm-thick slices for staining. To detect GFP expressing cells, we performed immunofluorescent staining using an anti-GFP (1:200, Santa Cruz Botechnology, Inc., CA, USA) for the primary antibody and an Alexa 488-conjugated goat anti-rabbit immunoglobulin-G (igG, 1:200; Invitrogen) the secondary antibody. The tissue slides were stained with 4,6-diamidino-2-phenylindole (DAPI, Vector Laboratories, Burlingame, CA), and were observed using fluorescence microscopy.

2.13. *Statistical analyses*

All results were calculated as means ± SEM or were expressed as a percentage of controls±SEM. GraphPad Prism software (GraphPad Software, San Diego, CA) was used for all the analyses. Significant differences in the assessment of the index were determined using the Mann–Whitney *U* test. The survival data are presented as Kaplan–Meier plots and analysed using a log-rank test. Significance was set at $p < 0.05$.

3. Results

3.1. *Characterisation and differentiation of hAT-MSCs*

The successfully cultured hAT-MSCs showed a fibroblast-like morphology in MSC expansion medium. These cells expressed CD73 (91.2%), CD90 (96.4%) and CD105 (75.4%), which are generally considered to be markers of MSCs, but they lacked the hematopoietic lineage markers CD14 (0.3%), CD34 (0.1%), and CD45 (0.1%). The mesenchymal differentiation potency of hAT-MSCs was assessed after culture in the induction media. The hAT-MSCs differentiated into adipocytes, chondrocytes and osteocytes: they showed lipid droplets on oil red O staining, chondrogenic pellets on alcian blue staining and calcium deposits on alizarin red S staining (Fig. 1A). The potential for neuronal differentiation was assessed by immunofluorescence staining. The hAT-MSCs exhibited a characteristic neurosphere formation in neurosphere induction media (Fig. 1B). In neuronal induction media, hAT-MSCs expressed high levels of the Tuj1, GFAP and O4, suggesting transdifferentiation into a neuronal lineage (Fig. 1B). Twenty-one days after neuronal induction, differentiation into neuronal, astrocytic, and oligodendrocytic lineages was approximately 35 ± 1%, 51 ± 3% and 14 ± 4%, respectively.

3.2. *Transfection of hAT-MSCs with rCE using nucleofection*

RT-PCR showed the expected 1751 bp band of the inserted rCE cDNA in hAT-MSC.rCE, but not in hAT-MSCs (Fig. 2A). GFP expression was observed 72 h after nucleofection by fluorescence microscopy (Fig. 2B). The percentage of GFP expression was 79.8% at 7 d after transfection and 89.7% immediately before *in vivo* injection (Fig. 2C).

3.3. *SN38 conversion activity of hAT-MSC.rCE*

Conversion of CPT-11 to SN-38 by hAT-MSC.rCE was confirmed in conditioned media by HPLC-MS/MS analysis. hAT-MSC.rCE produced 0.1 nM SN-38 at a CPT-11 concentration of 5 μM after 3 d of incubation (Fig. 2D). The production of SN-38 by hAT-MSCs was not detected.

3.4. *In vitro sensitivity of CPT-11*

The sensitivity of hAT-MSC.rCE to CPT-11 was compared to that of hAT-MSCs. hAT-MSCs and hAT-MSC.rCE were incubated and treated with or without CPT-11 at final concentrations in the range of 0–50 μM. The hAT-MSC.rCE cells showed increased sensitivity compared to hAT-MSCs (Fig. 3A). For example, hAT-MSC.rCE (64.5 ± 1.9%) showed a significant decrease in cell viability compared to hAT-MSCs (89.9 ± 3.1%) treated with 5 μM of CPT-11 ($p < 0.05$).

3.5. *In vitro therapeutic efficacy of hAT-MSC.rCE*

To confirm the cytotoxic effects of hAT-MSC.rCE, cell viability studies were done in a direct mixed coculture system. After CPT-11 treatment, F98 cells cultured in the presence of hAT-MSC.rCE cells showed more effective growth inhibition than F98 cells with the parental cell line hAT-MSCs: compared to control, decreased cell viability was 26 ± 6.6% in F98 cells with

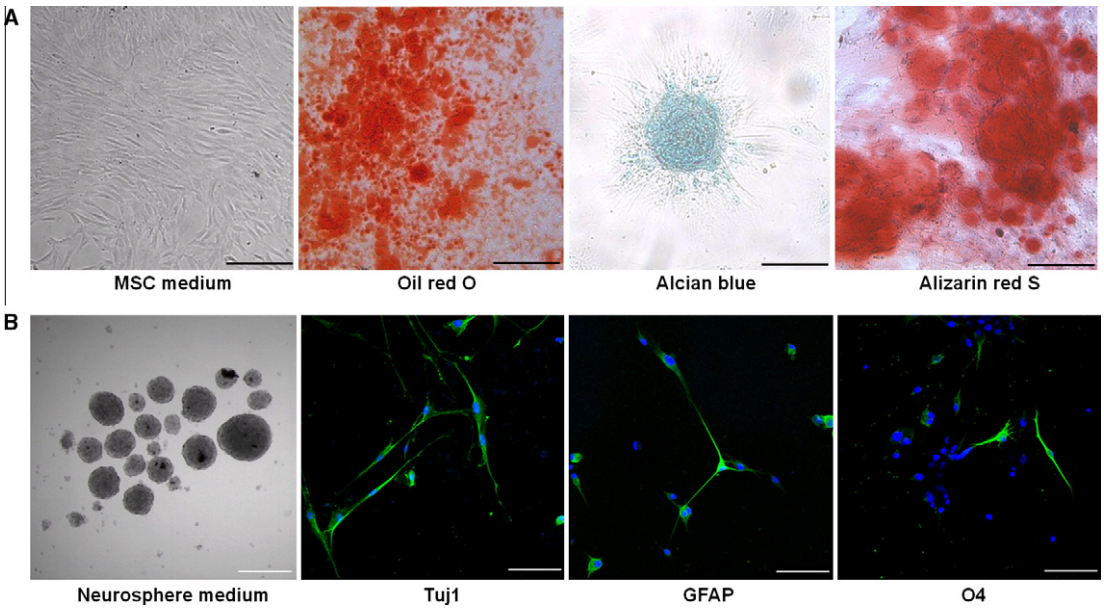

Fig. 1 – Multipotency of hAT-MSCs. (A) Mesenchymal differentiation of hAT-MSCs. In mesenchymal expansion medium, hAT-MSCs show fibroblast-like morphology. In mesenchymal induction medium, they differentiate into mesenchymal lineage. Differentiation of hAT-MSCs into adipocytes, chondrocytes and osteocytes were confirmed by oil red O, alcian blue, and alizarin red S staining, respectively. (B) Neuronal differentiation of hAT-MSCs. In neurosphere induction medium, hAT-MSCs produce neurospheres. In neuronal induction medium, hAT-MSCs express the neuronal lineage marker Tuj1, the astrocytic lineage marker GFAP, and the oligodendrocytic lineage marker O4 (green). The nuclei of differentiated cells were counterstained with DAPI (blue). Bars indicate 100 μm.

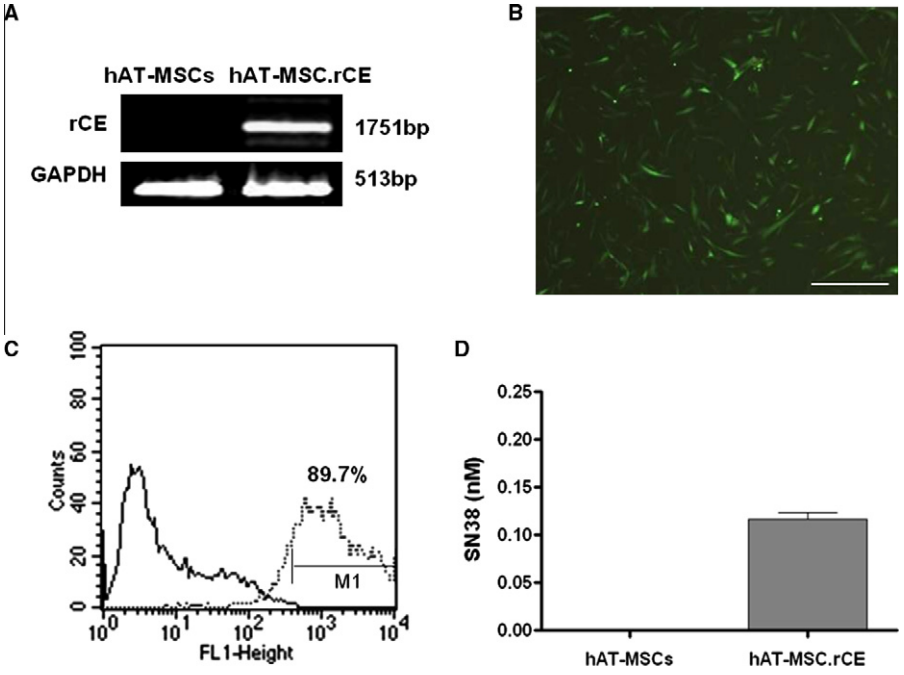

Fig. 2 – Confirmation of rCE expression in hAT-MSC.rCE after nucleofection. (A) Transcripts of rCE from hAT-MSCs and hAT-MSC.rCE were analysed by reverse transcription-PCR. GAPDH controls confirmed that equal amounts of cDNA were loaded. (B) Expression of GFP (green) was visualised by fluorescence microscopy 72 h after nucleofection. Bars indicate 100 μm. (C) Transfection efficiency was analysed using FACS analysis immediately before *in vivo* injection. (D) CPT-11 conversion activity shows that only hAT-MSC.rCE converted CPT-11 to SN38.

hAT-MSC.rCE versus 1.0 ± 7.5% in F98 cells with hAT-MSCs at the 5 μM of CPT-11 treatment, 63 ± 4.4% versus 26 ± 7.0% at 7 μM, and 85 ± 1.0% versus. 47 ± 3.0% at 10 μM ($p < 0.05$, Fig. 3B). These results indicate that hAT-MSC.rCE could

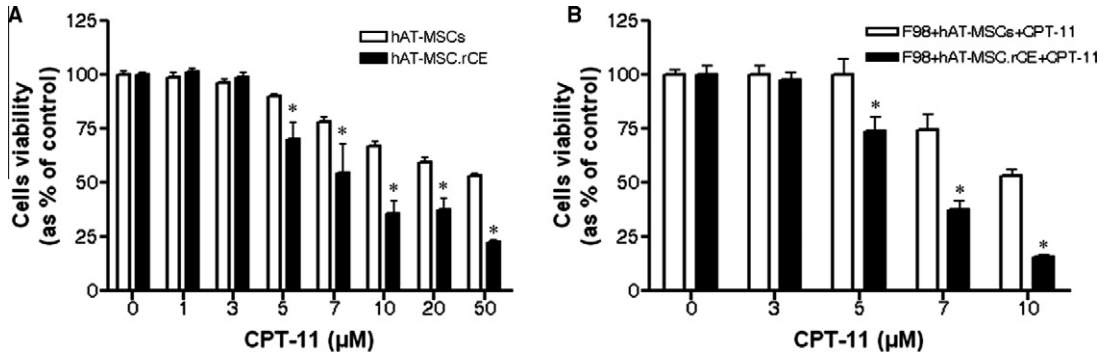

Fig. 3 – The bioactivity of CPT-11 and hAT-MSC.rCE system determined by cell viability assay. (A) Sensitivity of hAT-MSCs and hAT-MSC.rCE to CPT-11. hAT-MSC.rCE cells have increased sensitivity to CPT-11 compared to hAT-MSCs. (B) *In vitro* therapeutic efficacy of hAT-MSC.rCE. F98 cells cultured with hAT-MSC.rCE cells show more effective growth inhibition than cells with hAT-MSC cells after CPT-11 treatment. Columns, mean percentage of the control viability; bars, SE (*$p < 0.05$, Mann–Whitney *U* test).

convert sufficient amounts of CPT-11 to SN-38 to effectively kill F98 cells *in vitro*.

3.6. *Migratory ability of hAT-MSC.rCE*

The migratory capacity of hAT-MSCs and hAT-MSC.rCE was evaluated by migration assays. The migration ability of hAT-MSCs (OD value: 0.32 ± 0.001) and hAT-MSC.rCE (OD value: 0.30 ± 0.015) was higher than HFF-1 cells (OD value: 0.04 ± 0.001, $p < 0.0001$) in F98-conditioned medium (Fig. 4). The hAT-MSC.rCE cells showed no change of migratory ability compared to hAT-MSCs after rCE transfection.

3.7. *Long-term survival and histological analysis*

Our data showed that rats treated with hAT-MSC.rCE and CPT-11 (median survival, 24 d) and those treated with CPT-11 only (median survival, 19 d) survived significantly longer than rats treated with PBS (median survival, 15 d) or hAT-MSCs (median survival, 15 d; $p = 0.0004$). Rats treated with hAT-MSC.rCE and CPT-11 showed modestly longer survival than rats treated with CPT-11 only ($p = 0.0018$; Fig. 5).

In vivo studies showed that the majority of intracranially injected CM-DiI-labelled hAT-MSC.rCE cells localised to the tumour bed and the tumour-normal parenchyma interface (Fig. 5C). hAT-MSC.rCE cells also expressed GFP which was indirect evidence of the presence of rCE. We could not detect any abnormalities, including tissue damage in the brains of hAT-MSC.rCE-treated animals.

4. Discussion

Our results indicate that MSCs are easily isolated from human adipose tissue and characterised. As a proof-of-concept study, we demonstrated the therapeutic potential of a hAT-MSC-based prodrug gene therapy against brainstem glioma.

MSCs from human adipose tissues have the advantages of autologous stem cell transplantation. hAT-MSCs could be obtained from a child with a brainstem glioma and reintroduced into that patient after genetic engineering. Although cultured hMSCs do not fulfil stringent stem cell criteria compared to their *in vivo* precursors, they possess a number of intriguing properties, such as proliferation, differentiation capacities, stroma function and immunomodulatory properties that make them reasonable resources for cell-based therapy.[19–21] We successfully isolated and maintained abundant MSCs from human adipose tissue, which is available for clinical applications in large quantities. hAT-MSCs showed transdifferentiation into neuronal lineages in neuronal induction medium. The transdifferentiation efficiency of hAT-MSCs into neurons, astrocytes, and oligodendrocytes was 35% 51%, and

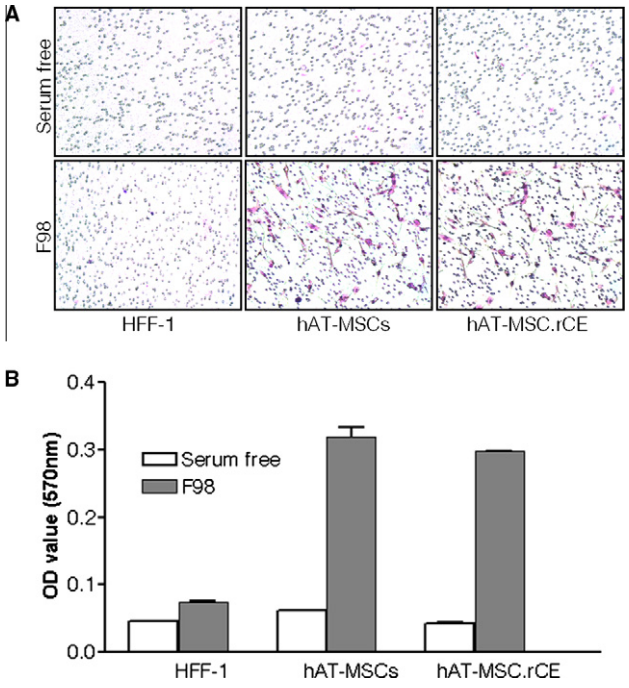

Fig. 4 – *In vitro* migration assays of hAT-MSCs and hAT-MSC.rCE towards brain tumour cells. hAT-MSCs and hAT-MSC.rCE migrated to F98 cells in conditioned medium more frequently than HFF-1 cells by 4-fold ($p < 0.05$, Mann–Whitney *U* test).

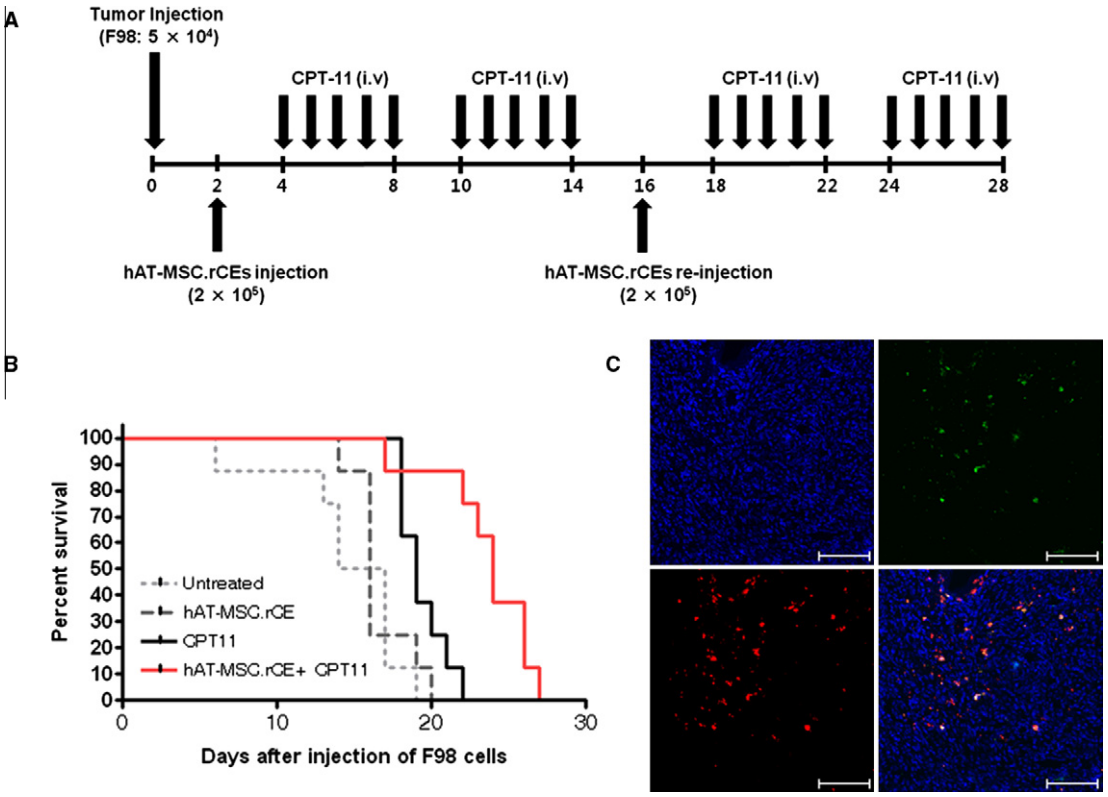

Fig. 5 – Antitumour effect of systemically administered hAT-MSC.rCE in the presence of CPT-11 *in vivo*. (A) Schematic representation shows that rats bearing brainstem gliomas received hAT-MSC.rCE 2 d later and then were treated with CPT-11 systemically though intravenous injection. Injection of hAT-MSC.rCE and CPT-11 were performed twice. (B) Kaplan–Meier plots and a log-rank test show prolonged survival in rats treated with hAT-MSC.rCE/CPT-11 compared to the other groups: hAT-MSC.rCE/CPT-11 versus PBS or hAT-MSCs, $p = 0.0004$; hAT-MSC.rCE/CPT-11 versus CPT-11, $p = 0.0018$. (C) The majority of intracranially injected CM-DiI-labeled hAT-MSC.rCE cells (red) localised to the tumour bed and expressed GPF protein (green). Sections were counterstained with DAPI (blue). Bars indicate 100 μm.

14%, respectively, which is comparable to other published data.[22–24] This transdifferentiation potential might not be an important issue in neuro-oncology; however, it might be important in neurodegenerative diseases such as Parkinson's disease and Alzheimer's disease.[25,26]

For gene therapy based on hMSCs, viral vectors have been utilised as major delivery systems because of their high efficiency compared to non-viral vectors.[27] However, viral vectors may create damaging immunological reactions by immune-mediated toxicity, especially in the presence of circulating antibodies to the viral vectors[27,28] or by triggering immune reactions to self- or transgene antigens.[27,29] Therefore, we used a non-viral transfection system for genetic modification of hAT-MSCs. The overall transfection efficacy was approximately 90%. Transfected cells were purified through FACS processing before *in vivo* transplantation. In the clinical setting, hAT-MSCs could be transfected and purified before each injection because of the simple isolation procedure and high yield.

CPT-11 is a prodrug activated by CE, which converts it to SN-38. Prodrugs are relatively non-toxic, inactive compounds delivered systemically and converted into biologically active cytotoxic agents only after reaching the target region.[30,31] A prodrug gene engineered into MSCs would provide protection from potential tumourigenesis by stem cells. In this study, hAT-MSCs were engineered to encode for rCE, a prodrug-converting enzyme, by nucleofection. Transfected rCE efficiently converted CPT-11 to SN38, resulting in a cytotoxic effect *in vitro*. After genetic engineering, the migration ability of hAT-MSCs towards the tumour was not changed. In the *in vivo* study, we administered the hAT-MSC.rCE to rats with brainstem gliomas and systemically treated them with CPT-11 by intravenous injection. The rats treated with hAT-MSC.rCE and CPT-11 survived 10 d longer than those treated with PBS or hAT-MSCs ($p = 0.0004$) and 5 d longer than those treated with CPT-11 but not hAT-MSC.rCE ($p = 0.0018$).

Though statistically significant, the actual increase in survival time was less than anticipated. This result may be due to the use of a suboptimal concentration of CPT-11. In addition, the possibility that CPT-11 may not be a very effective therapeutic agent against brainstem gliomas should be considered. CPT-11 is a potent chemotherapeutic drug against various systemic cancers, but it has been shown to be rather ineffective as a single agent in gliomas.[32] Prolonged survival has been reported as part of a multiagent regimen with anti-angiogenic agents in recurrent supratentorial high grade gliomas.[33] Still, the therapeutic effect of CPT-11 against brainstem glioma, even in combination with bevacizumab, is controversial; there are anecdotal case reports of the

successful control of the disease with CPT-11 and bevacizumb,[34] but clinical trials show no definite gain in survival.

This study is proof-of-concept for the therapeutic potential of hAT-MSCs for brainstem glioma. We suggest that hAT-MSCs can be used as cellular vehicles for prodrug gene therapy. Specific therapeutic genes should be identified, and the regimen for administering hAT-MSCs optimised in future studies.

Role of the funding source

No influence of scientific researches.

Conflict of interest statement

None declared.

Acknowledgements

This study was supported by the Korea Research Foundation Grant No. KRF-2006-312-E00117 and by grant from the Seoul National University Hospital Research Fund (03-2009-008). We thank CJ Cheiljedang Corp. for providing CPT-11.

REFERENCES

1. Okada H, Low KL, Kohanbash G, et al. Expression of glioma-associated antigens in pediatric brain stem and non-brain stem gliomas. *J Neurooncol* 2008;**88**:245–50.
2. Jennings MT, Freeman ML, Murray MJ. Strategies in the treatment of diffuse pontine gliomas: the therapeutic role of hyperfractionated radiotherapy and chemotherapy. *J Neurooncol* 1996;**28**:207–22.
3. Aboody KS, Brown A, Rainov NG, et al. Neural stem cells display extensive tropism for pathology in adult brain: evidence from intracranial gliomas. *Proc Natl Acad Sci USA* 2000;**97**:12846–51.
4. Benedetti S, Pirola B, Pollo B, et al. Gene therapy of experimental brain tumors using neural progenitor cells. *Nat Med* 2000;**6**:447–50.
5. Kim SK, Cargioli TG, Machluf M, et al. PEX-producing human neural stem cells inhibit tumor growth in a mouse glioma model. *Clin Cancer Res* 2005;**11**:5965–70.
6. Kim SK, Kim SU, Park IH, et al. Human neural stem cells target experimental intracranial medulloblastoma and deliver a therapeutic gene leading to tumor regression. *Clin Cancer Res* 2006;**12**:5550–6.
7. Menon LG, Kelly K, Yang HW, et al. Human bone marrow-derived mesenchymal stromal cells expressing S-TRAIL as a cellular delivery vehicle for human glioma therapy. *Stem Cells* 2009;**27**:2320–30.
8. Nakamizo A, Marini F, Amano T, et al. Human bone marrow-derived mesenchymal stem cells in the treatment of gliomas. *Cancer Res* 2005;**65**:3307–18.
9. Lee DH, Ahn Y, Kim SU, et al. Targeting rat brainstem glioma using human neural stem cells and human mesenchymal stem cells. *Clin Cancer Res* 2009;**15**:4925–34.
10. Bobis S, Jarocha D, Majka M. Mesenchymal stem cells: characteristics and clinical applications. *Folia Histochem Cytobiol* 2006;**44**:215–30.
11. Egusa H, Schweizer FE, Wang CC, Matsuka Y, Nishimura I. Neuronal differentiation of bone marrow-derived stromal stem cells involves suppression of discordant phenotypes through gene silencing. *J Biol Chem* 2005;**280**:23691–7.
12. Utsunomiya T, Shimada M, Imura S, et al. Human adipose-derived stem cells: potential clinical applications in surgery. *Surg Today* 2011;**41**:18–23.
13. Kucerova L, Altanerova V, Matuskova M, Tyciakova S, Altaner C. Adipose tissue-derived human mesenchymal stem cells mediated prodrug cancer gene therapy. *Cancer Res* 2007;**67**:6304–13.
14. Choi SA, Hwang SK, Wang KC, et al. Therapeutic efficacy and safety of TRAIL-producing human adipose tissue-derived mesenchymal stem cells against experimental brainstem glioma. *Neuro Oncol* 2011;**13**:61–9.
15. Chang DY, Yoo SW, Hong Y, et al. The growth of brain tumors can be suppressed by multiple transplantation of mesenchymal stem cells expressing cytosine deaminase. *Int J Cancer* 2010;**127**:1975–83.
16. Danks MK, Yoon KJ, Bush RA, et al. Tumor-targeted enzyme/prodrug therapy mediates long-term disease-free survival of mice bearing disseminated neuroblastoma. *Cancer Res* 2007;**67**:22–5.
17. Wierdl M, Morton CL, Weeks JK, et al. Sensitization of human tumor cells to CPT-11 via adenoviral-mediated delivery of a rabbit liver carboxylesterase. *Cancer Res* 2001;**61**:5078–82.
18. Jallo GI, Volkov A, Wong C, Carson Sr BS, Penno MB. A novel brainstem tumor model: functional and histopathological characterization. *Childs Nerv Syst* 2006;**22**:1519–25.
19. Baksh D, Song L, Tuan RS. Adult mesenchymal stem cells: characterization, differentiation, and application in cell and gene therapy. *J Cell Mol Med* 2004;**8**:301–16.
20. Bexell D, Scheding S, Bengzon J. Toward brain tumor gene therapy using multipotent mesenchymal stromal cell vectors. *Mol Ther* 2010;**18**:1067–75.
21. Dominici M, Le Blanc K, Mueller I, et al. Minimal criteria for defining multipotent mesenchymal stromal cells. The International Society for Cellular Therapy position statement. *Cytotherapy* 2006;**8**:315–7.
22. Anghileri E, Marconi S, Pignatelli A, et al. Neuronal differentiation potential of human adipose-derived mesenchymal stem cells. *Stem Cells Dev* 2008;**17**:909–16.
23. Safford KM, Hicok KC, Safford SD, et al. Neurogenic differentiation of murine and human adipose-derived stromal cells. *Biochem Biophys Res Commun* 2002;**294**:371–9.
24. Strem BM, Hicok KC, Zhu M, et al. Multipotential differentiation of adipose tissue-derived stem cells. *Keio J Med* 2005;**54**:132–41.
25. Safford KM, Rice HE. Stem cell therapy for neurologic disorders: therapeutic potential of adipose-derived stem cells. *Curr Drug Targets* 2005;**6**:57–62.
26. Heinrich AC, Patel SA, Reddy BY, Milton R, Rameshwar P. Multi- and inter-disciplinary science in personalized delivery of stem cells for tissue repair. *Curr Stem Cell Res Ther* 2009;**4**:16–22.
27. Pulkkanen KJ, Yla-Herttuala S. Gene therapy for malignant glioma: current clinical status. *Mol Ther* 2005;**12**:585–98.
28. Byrnes AP, Rusby JE, Wood MJ, Charlton HM. Adenovirus gene transfer causes inflammation in the brain. *Neuroscience* 1995;**66**:1015–24.
29. Zermansky AJ, Bolognani F, Stone D, et al. Towards global and long-term neurological gene therapy: unexpected transgene dependent, high-level, and widespread distribution of HSV-1 thymidine kinase throughout the CNS. *Mol Ther* 2001;**4**:490–8.
30. Altaner C. Prodrug cancer gene therapy. *Cancer Lett* 2008;**270**:191–201.

31. Aboody KS, Najbauer J, Danks MK. Stem and progenitor cell-mediated tumor selective gene therapy. *Gene Ther* 2008;**15**:739–52.
32. Prados MD, Lamborn K, Yung WK, et al. A phase 2 trial of irinotecan (CPT-11) in patients with recurrent malignant glioma: a North American Brain Tumor Consortium study. *Neuro Oncol* 2006;**8**:189–93.
33. Vredenburgh JJ, Desjardins A, Herndon 2nd JE, et al. Phase II trial of bevacizumab and irinotecan in recurrent malignant glioma. *Clin Cancer Res* 2007;**13**:1253–9.
34. Torcuator R, Zuniga R, Loutfi R, Mikkelsen T. Bevacizumab and irinotecan treatment for progressive diffuse brainstem glioma: case report. *J Neurooncol* 2009;**93**:409–12.